Vol 17 No 2, February 2008
1674-1056/2008/17(02)/0592-07
Chinese Physics B
© 2008 Chin. Phys. Soc.
and IOP Publishing Ltd

Excitation and decay dynamics of 1s2s inner-shell double-vacancy states of neon atoms*

Ding Xiao-Bin(丁晓彬)[a], Dong Chen-Zhong(董晨钟)[a,b,†], Fumihiro Koike[c], Takako Kato[d], and Stephan Fritzsche[e]

[a] *College of Physics and Electronic Engineering, Northwest Normal University, Lanzhou* 730070, *China*
[b] *Center of Theoretical Nuclear Physics, National laboratory of Heavy-Ion Accelerator of Lanzhou, Lanzhou* 730000, *China*
[c] *Physics Department, School of Medicine, Kitasato University*, 1-15-1 *Kitasato, 228-8555, Japan*
[d] *National Institute for Fusion Science, Nagoya*, 464-01, *Japan*
[e] *Department of Physics, University of Kassel, Heinrich-Plett-Straβe* 40, *D*-34132, *Kassel, Germany*

(Received 28 May 2007; revised manuscript received 20 August 2007)

The photo-excitation and Auger decay processes of inner-shell double vacancy states $1s2s2p^6(^{1,3}S)3s3p$ of neutral neon atoms have been studied theoretically. Multi-configuration Dirac–Fock (MCDF) calculations have been carried out, with electron correlation effects taken into consideration. The relaxation of core and excited orbitals and configuration interaction are found to be crucial to creating the double vacancy states by single photo-absorption. The predominant decay paths for the double vacancy states turn out to be of the LLM Auger decay to 1s $2s^22p^53s(3p)$, KLL Auger decay to $1s^22s2p^43s3p$, and KLM Auger decay to $1s^22p^63s(3p)$. They lead to further Auger decay, creating the neon ions of multiple charge states. For both double and single vacancy states the spectator type of Auger process is dominated in all the Auger decay processes. Theoretical Auger electron spectra are presented for further investigations, experimental and theoretical.

Keywords: correlation effects, multi-configuration Dirac–Fock (MCDF) method, Auger decay
PACC: 3120T, 3280H, 3270C

1. Introduction

Inner-shell excited states of atoms or ions can be created by the impact of photons, electrons, or ions on atoms or ions, and the states may decay either radiatively or non-radiatively. Among those processes, the dynamics of multiple electron excitation and the subsequent decay processes arose the great interest in the sense of studying the electron correlations or the break-down of the independent particle pictures in atomic excited states and their transition dynamics. We can find in the literature a number of studies on atomic multiple electron excitation processes.[1−15] However, most of those studies focused on the lighter atoms, and only a few investigations[10−15] that deal with multiple core-electron excitations above the outermost closed subshells can be found. In those systems, we may expect the relaxation of the residual and the outermost closed subshell electron orbitals to take place due to the creation of inner-shell double holes, which we may also call the effects of electron correlation. The photon impact study for this type of excitations has been made possible in the couple of decades owing to the development of advanced synchrotron radiation sources facilities and high-resolution spectroscopy methods. In contrast to the earlier work, for example, by Madden and Codling,[1−2] where only the photo double-electron excitation of helium atoms was observed, now the up-to-date technologies enable us to observe the co-operative motions of many electrons in double-electron excitations and their subsequent decays.

Recently, 1s2s and 1s2p double electron excitations of neon atoms have been studied extensively by several research groups[10−15] by means of photon absorption spectroscopy,[10−11] photoion spectroscopy[12−13] and resonant Auger electron spectroscopy.[14] They have given theoretical analy-

*Project supported by the National Natural Science Foundation of China (Grant Nos 10434100, 10774122), the Core-University Program between Japanese Society of Promotion of Science and Chinese Academy of Sciences, the Foundation of Center of Theoretical Nuclear Physics of National Laboratory of Heavy Ion Accelerator of Lanzhou, and the Foundation of Northwest Normal University (Grant No NWNU-KJCXGC-03-21).
†Corresponding author. E-mail: dongcz@nwnu.edu.cn

ses on [1s2s]$nln'l'$ or [1s2p]$nln'l'$ spectra, where the square brackets denote the hole configurations; nl and $n'l'$ represent the single electron orbitals with principal quantum numbers n and n' and orbital angular momenta l and l', respectively. Although their theoretical studies have been extensively carried out, the further calculations are still needed to gain a deep insight into the spectra. It is desired to make clear the mechanism of excitations of the states that are dipole unfavored in the independent particle framework. It is also interesting to investigate the Auger decay from the doubly excited states and subsequent Auger decay processes.

In the present paper, we perform a calculation of double-electron core-excited [1s2s](^{1,3}S)3s3p states including both the orbital relaxation effects and the most important configuration interaction (CI) effects. We further calculate the Auger rate to gain the representative decay paths of the excited states. In Section 2, we briefly introduce the methods in the present calculation. In Section 3, we discuss the dynamics; Section 3.1 is devoted to the excitation mechanism and Section 3.2 is given to the decay processes. Finally, in Section 4, we draw some conclusions from the present study and discuss the possible future prospects.

2. Theoretical method

We can use the GRASP92 program,[16] which is based on the multi-configuration Dirac–Fock method (MCDF),[17] to obtain the atomic state wavefunctions (ASFs) and the energies of the ground, core excited and final ionic states. The radiative or non-radiative transition matrix elements may be calculated by using the recently developed RATIP package.[18]

In the calculation, the radiation transition rate A^r_{ik} from the inner-shell excited state i to the radiative final state k can be obtained from the formula,[19]

$$A^r_{ik} = 2\frac{\omega}{c}|\langle\alpha_i(PJM)|P^{(1)}|\alpha_k(P'J'M')\rangle|^2, \quad (1)$$

where $\langle\alpha_i(PJM)|$ and $|\alpha_k(P'J'M')\rangle$ are the ASFs of the initial and final states with parities P and P', total angular momenta J and J', azimuthal components M and M', and residual quantum numbers α_i and α_k that specify the atomic state, respectively. The ASFs are given by a linear combination of configuration state wavefunctions (CSFs); $P^{(1)}$ is the electric dipole tensor operator; ω is the radiative photon energy; c is the speed of light in vacuum.

The oscillator strength f_{ik} corresponding to the radiation transition may be obtained from the following formula:

$$f_{ik} = \frac{c^3}{2\omega^2}A^r_{ik}. \quad (2)$$

The Auger decay rate A^a_{if} from the inner-shell doubly excited state i to the Auger final state f can be calculated by using the following formula:

$$A^a_{if} = 2\frac{\omega}{c}\left|\langle\alpha_i(PJM)|\sum_{s<t}\frac{1}{r_{s,t}} + V_{\rm B}|\alpha_f(P''J''M'')\rangle\right|^2, \quad (3)$$

where $\langle\alpha_i(PJM)|$ is the ASF of initial state, while $|\alpha_f(P''J''M'')\rangle$ is the ASF of Auger final state which can be constructed by the CSFs of ionic states and the continuum wavefunction of Auger electron, which is solved by including the exchange effects with the ionic wavefunctions; $\frac{1}{r_{s,t}}$ is the operator of Coulomb interaction between the sth electron and tth electron; $V_{\rm B}$ is the Breit interaction operator.

According to the energy conservation law, the kinetic energy $E_{\rm A}$ of Auger electron is given by the difference between the energy E_i of the initial state i and the energy E_f of the final ionic state f.

3. Results and discussion

3.1. Generation of the inner-shell doubly excited states

When a photon is absorbed or emitted during transition, the charge density distribution of atomic ions will change. This is referred to as the orbital relaxation. The radial charge density distributions of the ground configuration and inner-shell doubly excited/ionized configurations of neon atoms/ions are given in Fig.1. Owing to the excitation/ionization of two inner-shell electrons, the charge density distribution change dramatically and turns different from that of the ground state. It is clearly shown in Fig.1 that there is a prominent change in inner-shell charge distribution between the ground state and the double inner-shell excited states of neutral neon. At the same time, the outer part of the charge distribution of inner-shell doubly excited states extends towards larger radial distance. For the inner regions of the double inner-shell excitation and ionization states, it can also be found from the figure that the charge density

distributions for the two cases are almost the same. It is reasonable that the screening effects from outer shell electrons have little influence on the charge density distributions of inner shell electrons, which accords with our previous results.[22−24]

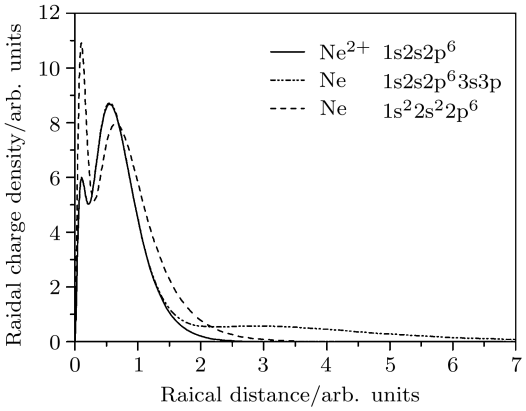


Fig.1. Comparison among the calculated charge density distributions of $Ne^{2+}1s2s2p^6$, $Ne1s2s2p^63s3p$ and $Ne1s^22s^22p^6$ configurations. The solid line is for the case of $Ne^{2+}1s2s2p^6$, while the dot-dashed line is for the charge density of $Ne1s2s2p^63s3p$ configuration, and the dashed line is for the case of ground state $Ne1s^22s^22p^6$.

The creation of the inner-shell vacancies leads to the redistribution of charge densities in configuration. In order to investigate it in detail, the values of mean orbital radii for the ground state, doubly inner-shell excited state of neutral neon and doubly ionization state of Ne^{2+} are all listed in Table 1. It can be found that the mean orbital radii of inner-shell doubly excited state are quite different from those of the ground state, but very close to those of Ne^{2+} ions. The orbital radii of inner-shell doubly excited state should contract dramatically after the creation of the inner-shell holes because of the increase of the effective nuclear charge. While, due to the difference in orbital between doubly excited and doubly ionized states, the wavefunctions of 3s and 3p electrons will screen the nuclear charge partly, and the effective nuclear charge will decrease a little because of the inner-shell electrons. These influences are so weak that the 1s orbital radii of doubly excited neutral neon remain almost unchanged. For the electrons in $2p_-$, 2p and 2s orbitals of neutral neon, due to the screening effects from the outer 3s and 3p electrons, their mean orbital radii are a little larger than those of Ne^{2+} ions. On the other hand, there can be found just a little influence on orbital features of inner-shell electrons when an outer shell electron is excited.[22] In contrast, the inner-shell excitation/ionization will influence the orbital characters of all orbitals including itself dramatically. Therefore, it is appropriate to estimate the relevant inner-shell orbital of inner-shell doubly excited state, based on that for Ne^{2+} ionic state.

Table 1. The mean orbital radii (in units of Bohr radius, a_0) for the relevant single electron orbitals of $1s^2$ $2s^2$ $2p^6$ and $1s2s2p^63s3p$ of neutral neon and Ne^{2+} ions.

ion	configuration	$\langle r\rangle_{1s}$	$\langle r\rangle_{2s}$	$\langle r\rangle_{2p_-}$	$\langle r\rangle_{2p}$	$\langle r\rangle_{3s}$	$\langle r\rangle_{3p_-}$	$\langle r\rangle_{3p}$
Ne	$1s^22s^22p^6$	0.158	0.890	0.966	0.963			
Ne^{2+}	$1s2s2p^6$	0.155	0.782	0.749	0.750			
Ne	$1s2s2p^63s3p$	0.155	0.792	0.751	0.753	3.449	4.039	4.039

As mentioned above, the electrons in the ground state and the inner-shell excited states of neutral neon will experience very different potentials due to the redistribution of the charge densities. Therefore, the orbital wavefunctions of the initial and final states must be optimized separately to include the orbital relaxation effects. As a result, the wavefunctions of the initial and final states will no longer orthogonal strictly. To incorporate the effects of this nonorthogonality into the computation of transition amplitudes, the overlap integral between the relevant orbitals in initial and final states must be included in the evaluation of the many-electron matrix elements. Recently, two computational modules CESD[20] and REOS99[21] have been developed by Fritzsche *et al* on the basis of the matrix expressions as derived by Löwdin.[25] These modules were designed to obtain the transition properties by expanding the atomic states in a Slater determinant basis via CESD module through using the wavefunctions from the GRASP92 package.[16]

The process of generating inner-shell doubly excited states is a multi-electron excitation process, and this process is always considered as the consequence of the electron correlation effects. In practical calculations, the electron correlation effects are taken into account by including the CI and orbital relaxation effects. The CI effects are considered in this work by including several important reference con-

figurations, while the relaxation effects are included by optimizing the orbital wavefunctions for the initial and final states separately. And we further include the overlap integral in the calculation of the transition matrix element. To find out which effect is dominant in this process, the CI and relaxation effects have been included in our calculation separately. In Table 2, we list the resonance energies and absorption oscillator strengths for the strong lines from ($1s^2$ $2s^2 2p^6)_{J=0}$ state to ($[1s2s]2p^6 3sn$p, 3p$ns)_{J=1}$ states with oscillator strengths greater than 1×10^{-5}. At first, we can see from Table 2 that if relaxation effects are taken into account, the good agreement with previous results can be achieved. Then, to include the relaxation effect together with CI effect, we optimize the orbital wavefunctions of the initial and final states separately, and include the CI effects from the two electron excitation configurations, such as 3snp ($n = 3, 4, 5, 6$), 3pns ($n = 4, 5, 6$) and 3p3d for the inner-shell doubly excited configuration $[1s2s]2p^6 3s3p$; $1s^2 2s^2$ $2p^4 3p^2$, $1s^2 2s 2p^5 3s 3p$, and $1s^2 2s^2 2p^4 3d^2$ for the low-lying ground state. It can also be seen from Table 2 that the CI effect also makes an important contribution to the oscillator strength. According to our results, the relaxation effect and CI effect can lead to this kind of multi-electron excitation process. Therefore, to some extent, this excitation process can be regarded as a 2s electron shaking up to 3s orbital accompanied by the 1s→3p resonance excitation.

Table 2. The excitation energy E (in eV) and absorption oscillator strength (gf) (in 10^{-4}) for the doubly excited states $([1s2s](^{3,1}S)3sn$p, 3p$ns)_{J=1}$.

	This work				Kato *et al*[13]	Oura *et al*[12]				Prince *et al*[15]	
Our	Relax.		Relax.+ CI		Energy	Energy		gf	Main	Energy	Assignment
Designation	E^*	gf	E	gf		Exp.	Cal.		configuration		
(^{3}S)3s3p	924.84	1.588	924.87	2.366	924.84	924.78	924.86	2.423	(^{3}S)3s3p	924.7	(^{3}S)3s3p
(^{3}S)3s4p			928.09	0.407	928.09	928.10	928.13	0.427	(^{3}S)3s4p	927.8	(^{3}S)3s4p
(^{3}S)3s5p			928.85	0.128			928.90	0.174	(^{3}S)3s5p		
(^{3}S)3s6p			929.19	0.045			929.23	0.080	(^{3}S)3s6p		
(^{3}S)3p4s			930.57	0.188	930.64	930.71	930.57	0.237	(^{3}S)3p4s	930.4	(^{3,1}S)3snl
(^{3}S)3p5s			931.68	0.099	931.81		931.68	0.109	(^{3}S)3p5s	931.6	(^{3,1}S)nln'l'
(^{3}S)3p6s			932.12	0.042	932.44		932.12	0.053	(^{3}S)3p6s	932.3	(^{3,1}S)nln'l'
(^{1}S)3s3p	935.21	0.854	934.79	0.684			934.57	0.466	(^{1}S)3s3p		
(^{1}S)3s4p			936.35	0.152							
(^{1}S)3s5p			936.89	0.136							
(^{1}S)3p4s			939.09	0.340							
(^{1}S)3p5s			939.96	0.174							

*The calculated energy are shifted by 0.2 eV towards lower energies.

3.2. Decay processes of $\{[1s2s](^{3,1}S)3s3p\}_{J=1}$ state

The inner-shell excited states lie in high energy regions and can decay by radiative and Auger transitions. For lower charged light ions, the most important decay process is Auger decay, while the radiative decay is negligible. Figure 2 shows the most important and possible first-step Auger decay channels and the subsequent Auger decay channels for $[1s2s](^{3,1}S)2p^6 3s3p$ states of neutral neon.

For the first-step Auger decay processes from the inner-shell double hole states, we include the main LLM Coster–Kronig, KLL and KLM Auger transitions in our calculation. Although the KLL and LLM

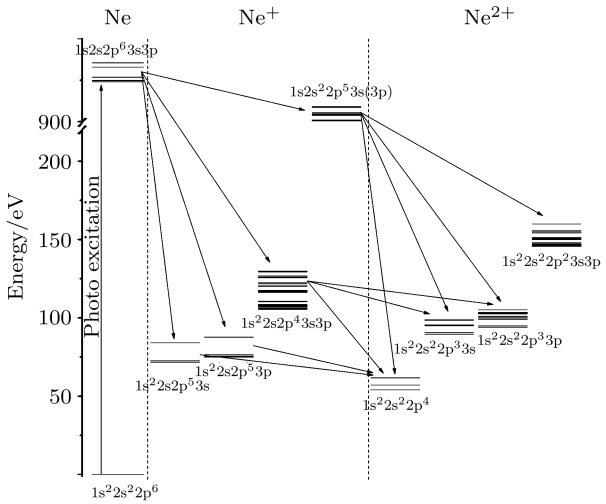


Fig.2. Important first-step and second-step Auger decay paths for the $\{[1s2s](^{3,1})3s3p\}_{J=1}$ inner-shell doubly excited states of neon atoms.

Auger decay processes accompanied with the excitation of an 3s(3p) electron to 4s(4p) orbital can make some minor contributions to the decay of [1s2p] double hole states,[14] we neglect them here to avoid the possibly complicating the calculation to some extents. Such calculation involve not only the continuum wave functions for the outgoing Auger electrons but also the electronic configurations of four open shells. Other possible decay channels such as $1s^22p^63s(3p)$, which can make a little contribution to the total Auger rate, are neglected in the present calculation. In the approximation, the theoretical Auger decay spectra are shown in Fig.3. According to our calculations, the LLM Coster-Kronig transition to the final state $1s2s^22p^53p(3s)$ is a main decay channel, while the final states $1s^22s2p^43s3p$ and $1s^22s2p^53s(3p)$ are also important, which accords with other results about the single inner-shell resonance Auger transition in which the LLM Coster–Kronig is also a dominant channel.[27] It can be expected that the Auger spectrum should be observed in an energy range shown in Fig.3.

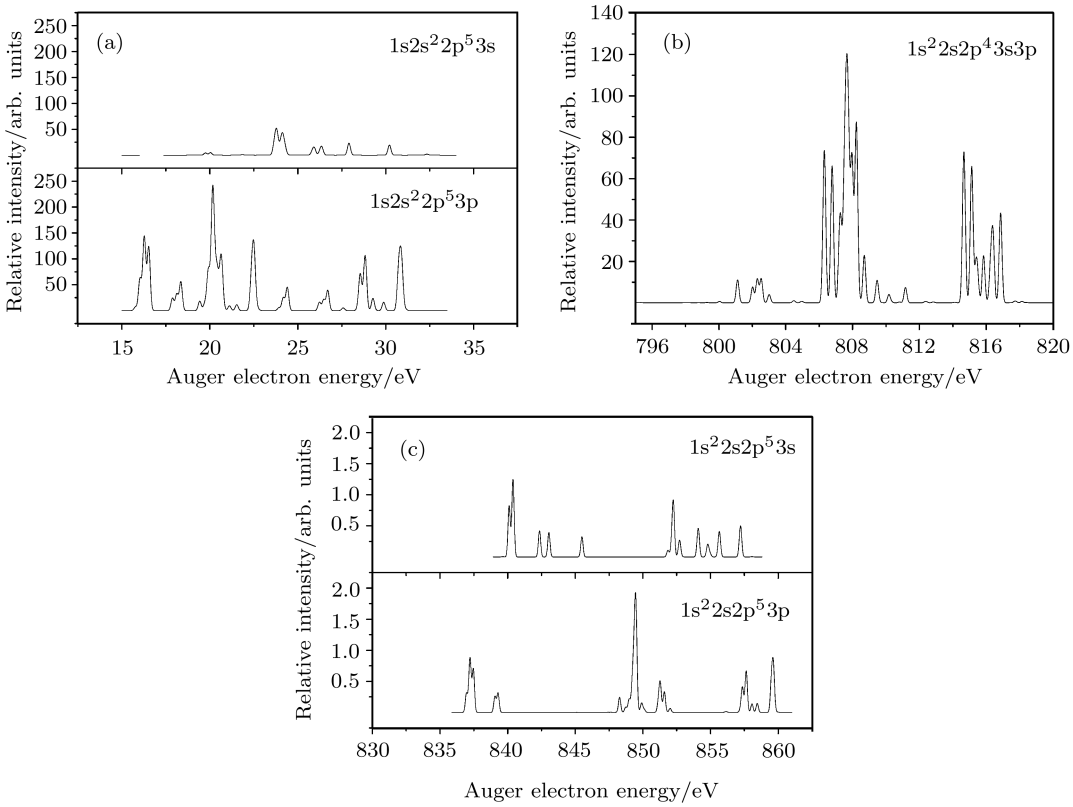


Fig.3. Theoretical Auger spectra of the double inner-shell excited states. Each line is convoluted with a 0.3 eV FWHM Gaussian profile factor. (a) Theoretical LLM Coster–Kronig Auger spectrum in an energy range from 16 to 32 eV for different final states. (b) Theoretical KLL Auger spectrum in an energy range from 800 to 815 eV for final states $1s^22s2p^43s3p$. (c) Theoretical KLM Auger spectrum in an energy range from 835 to 860 eV for different final states.

The final states of the first-step Auger decay process are still the hole states, which can undergo further Auger decays spontaneously. These are the so-called second-step Auger decay or subsequent Auger decay. The investigation of this process is helpful to diagnosing the dynamics of preceding processes. In this process all the important final states, such as $1s^22s^22p^4$, $1s^22s^22p^33s(3p)$ and $1s^22s^22p^23s3p$, are taken into account. The theoretical second-step Auger spectra are given in Fig.4, where the full width at half maximum (FWMH) is taken as 0.3 eV. It can be concluded from Fig.4 that the Auger decay to the excited states of Ne^{2+} ($1s^22s^22p^33s(3p)$) is stronger than to the ground state of Ne^{2+}. It is expected that most of the final ions observed in the ion yield spectra are in $1s^22s^22p^33s(3p)$ states. It can also be found in Figs.3 and 4 that the most prominent Auger transitions of both double hole and single hole states are of the spectator type Auger transitions.

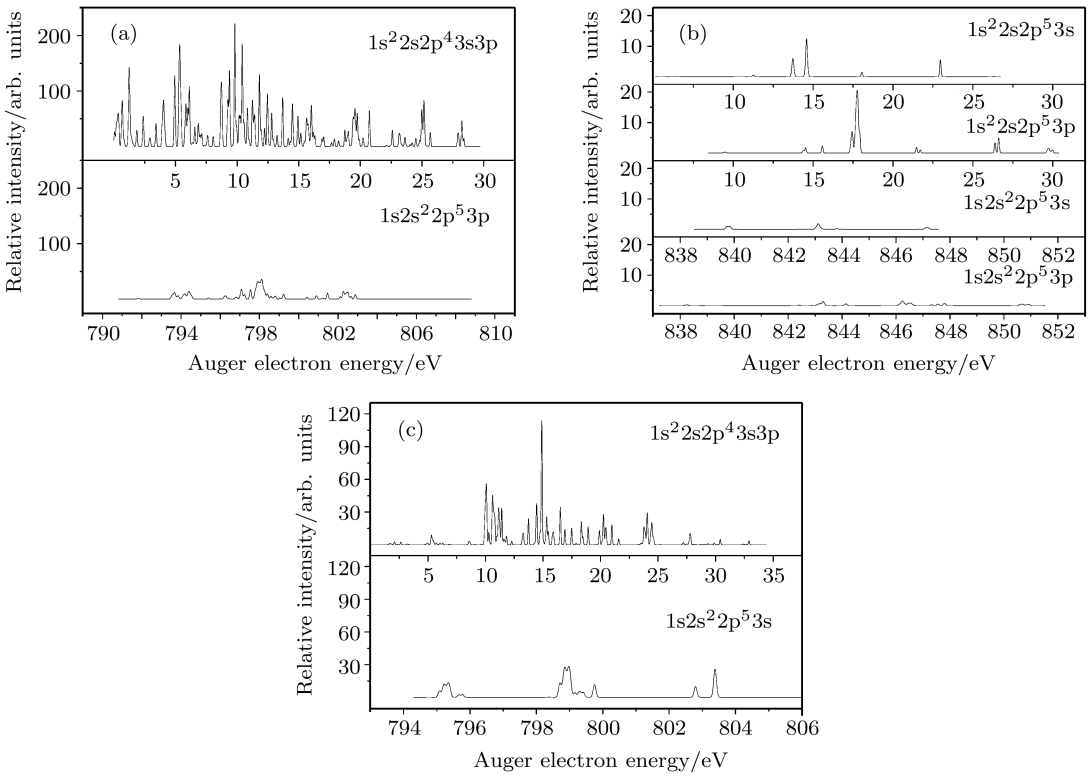


Fig.4. Theoretical Auger spectra of the second-step Auger decay process. Each line is convoluted with a 0.3 eV FWHM Gaussian profile factor. (a)Theoretical Auger spectrum from different initial states to the final state $1s^22s^22p^33p$. (b)Theoretical Auger spectrum from different initial states to the final state $1s^22s^22p^4$. (c)Theoretical Auger spectrum from different initial state to the final state $1s^22s^22p^33s$.

4. Conclusion

The excitation and the Auger decay of the inner-shell double hole states [1s2s]3s3p of neutral neon atoms have been studied by using the multi-configuration Dirac-Fock (MCDF) method. Our results indicate that the formation mechanism of the inner-shell double hole states can be understood as an inner-shell resonance excitation accompanied by a shaking-up process. Furthermore, the first-step Auger processes from the inner-shell double hole states and the subsequent Auger decay process are also studied. It is found that the LLM, KLL, KLM Auger decay processes from the inner-shell double hole states, respectively, to the final states $1s2s^22p^53p(3s)$, $1s2s^22p^53s(3p)$ and $1s^22s2p^43s3p$ are dominant in all the decay channels; while the subsequent Auger decay processes results mostly from the transitions to final states $1s^2\ 2s^22p^4$ and $1s^22s^22p^33s(3p)$. The present study will be helpful for further experimental and theoretical investigations into the inner-shell doubly excited states.

References

[1] Madden R P and Codling K 1963 *Phys. Rev. Lett.* **10** 516
[2] Madden R P and Codling K 1965 *Astrophys. J.* **141** 364
[3] Domke M, Schulz K, Remmers G, Kaindl G and Wintgen D 1996 *Phys. Rev.* A **53** 1424
[4] Kiernan L M, Kennedy E T, Mosnier J P, Costello J T and Sonntag B F 1994 *Phys. Rev. Lett.* **72** 2359
[5] Azuma Y, Koike F, Cooper J W, Nagata T, Kutluk G, Shigemasa E, Wehlitz R and Sellin I A 1997 *Phys. Rev. Lett.* **79** 2419
[6] Diehl S, Cubaynes D, Wuilleumier F J, Bizau J M, Journel L, Kennedy E T, Blancard C, VoKy L, Faucher P, Hibbert A, Berrah N, Morgan T J, Bozek J and Schlachter A S 1997 *Phys. Rev. Lett.* **79** 1241
[7] Menzel A, Frigo S P, Whitfield S B, Caldwell C D, Krause M O, Tang J Z and Shimamura I 1995 *Phys. Rev. Lett.* **75** 1479
[8] Xiong Zhuang and Bacalis N C 2007 *Chin. Phys.* **16** 374
[9] Hu Hongwei and Dong Chenzhong 2006 *Acta Phys. Sin.* **55** 6326 (in Chinese)

[10] Esteva J M, GauthéB and Dhez P 1983 *J. Phys. B: At. Mol. Opt. Phys.* **16** L263
[11] Avaldi L, Camilloni R, Stefani G, Comicioli C, Zacchigna M, Prince K C, Zitnik M, Quaresima C, Ottaviani C, Crotti C and Perfetti P 1996 *J. Phys. B: At. Mol. Opt. Phys.* **29** L737
[12] Oura M, Yamaoka H, Senba Y, Ohashi H and Koike F 2004 *Phys. Rev.* A **70** 062502
[13] Kato M, Morishita Y, Koike F, Fritzsche S, Yamaoka H, Tamenori Y, Okada K, Matsudo T, Gejo T, Suzuki I H and Saito N 2006 *J. Phys. B: At. Mol. Opt. Phys.* **39** 2059
[14] Oura M, Tamenori Y, Kanai Y, Yoshii H, Tsukamoto K and Koike F 2004 *Phys. Rev.* A **70** 022710
[15] Prince K C, Avaldi L, Sankari R, Richter R, Simone M and Coreno M 2005 *J. Elec. Spec. Rel. Phenom.* **144-147** 43
[16] Märtensson N, Svensson S and Gelius U 1987 *J. Phys. B: At. Mol. Opt. Phys.* **20** 6243
[17] Parpia F A, Fischer C F and Grant I P 1996 *Compt. Phys. Commun.* **94** 249
[18] Grant I P, McKenzie B J, Norrington P H, Mayers D F and Pyper N C 1980 *Comput. Phys. Commun.* **21** 207
[19] Fritzsche S 2001 *J. Elec. Spec. Rel. Phenom.* **114-116** 1155
[20] Grant I P 1974 *J. Phys. B: At. Mol. Opt. Phys.* **7** 1458
[21] Dong C Z and Fritzsche S 2005 *Phys. Rev.* A **72** 012501
[22] Dong C Z, Fritzsche S and Fricke B 2006 *Eur. J. Phys. D* **40** 317
[23] Li J, Dong C Z and Xie L Y 2006 *Acta Phys. Sin.* **55** 0655 (in Chinese)
[24] Fritzsche S and Grant I P 1995 *Compt. Phys. Commun.* **92** 111
[25] Fritzsche S, Fischer C F and Dong C Z 2000 *Compt. Phys. Commun.* **124** 340
[26] Löwdin P O 1955 *Phys. Rev.* A **97** 1474
[27] Axelrod T S 1976 *Phys. Rev.* A **13** 376